Published in final edited form as:
Structure. 2014 October 7; 22(10): 1520–1527. doi:10.1016/j.str.2014.08.009.

The structure of a conserved Piezo channel domain reveals a novel beta sandwich fold

Aron Kamajaya[a,b], **Jens Kaiser**[b,c], **Jonas Lee**[b,d], **Michelle Reid**[b], and **Douglas C. Rees**[b,d,*]

[a]Biochemistry and Molecular Biophysics Graduate Option, California Institute of Technology, Pasadena, CA 91125 USA

[b]Division of Chemistry and Chemical Engineering, California Institute of Technology, Pasadena, CA 91125 USA

[c]Beckman Institute, California Institute of Technology, Pasadena, CA 91125 USA

[d]Howard Hughes Medical Institute, California Institute of Technology, Pasadena, CA 91125 USA

Summary

Piezo has recently been identified as a family of eukaryotic mechanosensitive channels composed of subunits containing over 2000 amino acids, without recognizable sequence similarity to other channels. Here, we present the crystal structure of a large, conserved extramembrane domain located just before the last predicted transmembrane helix of *C. elegans* PIEZO, which adopts a novel beta sandwich fold. The structure was also determined of a point mutation located on a conserved surface at the position equivalent to the human PIEZO1 mutation found in Dehydrated Hereditary Stomatocytosis (DHS) patients (M2225R). While the point mutation does not change the overall domain structure, it does alter the surface electrostatic potential that may perturb interactions with a yet-to-be identified ligand or protein. The lack of structural similarity between this domain and any previously characterized fold, including those of eukaryotic and bacterial channels, highlights the distinctive nature of the Piezo family of eukaryotic mechanosensitive channels.

Introduction

The ability to translate environmental cues (chemical, electrical, and mechanical) into intracellular signals is crucial to the functioning of all cells. Although membrane protein receptors for many of these environmental signals have been identified, our understanding of the receptors for mechanical signal transduction remains incomplete. The best characterized models of mechanotransduction are bacterial mechanosensitive (MS) channels that protect cells from osmotic downshock (Levina et al., 1999). In multicellular eukaryotes,

*Correspondence to: Douglas C. Rees, Division of Chemistry and Chemical Engineering, MC 114-96, California Institute of Technology, 1200 East California Blvd., Pasadena, CA 91125. Phone: (626) 395-8393. Fax: 626-744-9524. dcrees@caltech.edu.

mechanosensitive channels are proposed to be involved in diverse physiological and developmental processes, such as somatosensory and auditory detection, change in blood osmolarity, muscle stretch, and others (Chalfie, 2009). The identity of the MS channels involved in these physiological processes remains contentious, however.

A notable exception to the unknown molecular identities of eukaryotic mechanosensors is provided by the Piezo family of mechanosensitive channels (Coste et al., 2012). Piezo was first identified through an siRNA knock-down screen and was shown to be necessary and sufficient for mechanically-activated currents (Coste et al., 2010). Piezos have been found in both multicellular and unicellular eukaryotes with the exception of yeast (Coste et al., 2010; Prole and Taylor, 2013). A striking characteristic of Piezo is the significant size, with all characterized homologs (human, mice, and Drosophila) containing over 2000 amino acids; moreover, mouse PIEZO1 has been demonstrated to form a tetrameric complex corresponding to a total molecular weight for the channel of ~1 MDa (Coste et al., 2012). No sequence similarities have been recognized between Piezo and other types of channels, nor have internal sequence repeats within the Piezo subunit been detected. PIEZO1 can be inhibited by a general blocker of mechanosensitive channels, GsMTx4 (Bae et al., 2011), and is shown to be sensitive to ruthenium red (Coste et al., 2010; Coste et al., 2012). Piezo channels are involved in several physiological processes, such as maintaining normal cell density in zebrafish and mammalian epithelial tissue (Eisenhoffer et al., 2012), mediating mechanical nociception in *Drosophila* larvae (Kim et al., 2012), and light touch in Rohon-Beard neurons in zebrafish (Faucherre et al., 2013). In humans, point mutations in PIEZO1 have been identified in patients suffering from Dehydrated Hereditary Stomatocytosis (DHS), an autosomal dominant hemolytic anemia disease (Zarychanski et al., 2012; Albuisson et al., 2013; Andolfo et al., 2013). In addition, inactivation of PIEZO1 in lung epithelial cells causes integrin-independent amoeboid cell migration (McHugh et al., 2012).

Understanding the gating mechanism of Piezo will enrich our current knowledge of how mechanical cues are converted into intracellular signals. A challenge in developing a gating model for Piezo arises from the absence of any structural information on the channel. Both the large size and the eukaryotic nature of Piezo create formidable technical challenges to the direct crystallographic analysis of the intact channel. The substantial size suggests, however, that the channel likely consists of smaller domains that may be more amenable to study. Here, we present the crystal structure at 2.5 Å resolution of a Piezo channel soluble domain designated CTL2 (C-Terminal Loop 2), located just before the last transmembrane helix and the C-terminal tail. This loop is predicted to be the largest soluble domain that is conserved across Piezo homologs. Moreover, there is accumulating evidence that the C-terminal portion of Piezo, including the CTL2, is involved in the gating kinetics of the channel. One of the human PIEZO1 point mutants found in DHS patients (M2225R) maps onto this loop and is shown to exhibit a delayed activation as well as slower inactivation (Bae et al., 2013a). A combination of a naturally-occurring mutation (M2225R) and an artificial mutation (R2456K in the C-terminal loop following the last transmembrane helix) in a human PIEZO1 double mutant construct eliminates the inactivation of the channel (Bae et al., 2013b). We also present the structure of *C. elegans* PIEZO CTL2 domain carrying a point mutation (M31R) at the equivalent position to the mutation found in DHS patients

(M2225R). These structures establish that CTL2 adopts a novel beta sandwich fold, and the absence of structural similarity between this domain and any previously characterized fold, including those of eukaryotic and bacterial channels, serves to highlight the distinctive nature of the Piezo family of eukaryotic mechanosensitive channels.

Results

Construct selection

As a starting point for structural analysis of the Piezo channel, we targeted large, well-conserved extramembrane loops. To gain a broad overview of the threading of Piezo protein through the membrane, we used multiple topology prediction webservers: TMHMM2 (Sonnhammer et al., 1998), Phobius (Kall et al., 2007), TOPCONS (Bernsel et al., 2009), TMPred (Hofmann and Stoffel, 1993), and SMART (Schultz et al., 1998). Although similar trends were evident, different algorithms predicted different numbers of transmembrane helices (between 30 and 40) for all characterized Piezos and there were differences in the predicted orientation of some of the extramembrane loops (Fig. 1). For our structural study, we selected a Piezo loop that satisfied the following criteria:

1. it is consistently predicted by all the topology-prediction algorithms used,
2. it is larger than 100 amino acid residues,
3. it is conserved across the Piezo family.

Under these constraints, we identified a predicted soluble domain corresponding to mouse PIEZO1 residues 2210 – 2453. These residues form an extramembrane loop preceding the last predicted transmembrane helix that we designate as the C-terminal loop 2 (CTL2) domain. The orientation of CTL2 could not be conclusively defined by the bioinformatics analysis, although 3 of the 4 topology prediction webservers predict that this domain is located in the extracellular environment (Fig. 1). An alignment of Piezo homologs using MAFFT (Fig S1; (Katoh et al., 2002)) reveals that CTL2 contains over 200 amino acid residues with a calculated molecular weight between 24 – 32 kDa, making CTL2 the largest conserved loop among the predicted loops of the Piezo channel. In addition, the Phyre2 webserver (Kelley and Sternberg, 2009) predicts that CTL2 has well-defined secondary structure (Fig S2). Therefore, we selected CTL2 for crystallographic analysis.

Architecture of the *C. elegans* CTL2 domain

Following a screen of various Piezo orthologues (see Materials and Methods), the *C. elegans* CTL2 domain was found to be amenable for crystallographic analysis. The structure of wild type *C. elegans* CTL2 establishes that this domain is organized around a core of three beta sheets flanked by two pairs of helices with overall dimensions of ~60 Å × 40 Å × 30 Å (Fig 2). The secondary structure observed in the crystal structure generally matches that predicted by the Phyre2 webserver (Fig S2). The three beta sheets are arranged such that sheet 1 (strands 1, 2, 5, 6, with strands numbered from the N-terminus) is nearly parallel to sheet 2 (strands 3, 4, 11, 8), and perpendicular to sheet 3 (strands 7, 9, 10).

To identify whether any protein of known structure shares a similar fold with CTL2, we used SSM (Krissinel and Henrick, 2004) as well as the DALI server (Holm and Rosenstrom, 2010) to perform a structure-based alignment. None of the identified proteins exhibited close similarities to CTL2 (Max z-score: 2.8). Most of these candidate proteins possess a beta sandwich fold composed of two beta sheets; this is different than our Piezo soluble domain structure that consists of three beta sheets. However, if we consider sheet 1 and sheet 2 of CTL2 as the beta sandwich core with the rest of the protein as connectors, we obtain a two beta sheet sandwich core with a 2D connectivity diagram illustrated in (Fig S3a). A comparison between the Piezo loop structure and the identified proteins did not reveal any significant connectivity similarity (Fig S3b). Subsequently, we explored the structural classification database CATH (Sillitoe et al., 2013) for two-sheet beta sandwich containing proteins (CATH ID: 2.60). Examination of the strand order in the beta sheets of these proteins failed to identify any close matches between CTL2 and previously solved structures. Therefore, we conclude that Piezo C-terminal soluble domain exhibits a novel beta sandwich fold.

Regions of potential functional significance were identified from the patterns of residue conservation evaluated with the programs ProFunc (Laskowski et al., 2005a, b) and ConSurf (Ashkenazy et al., 2010). Both programs identified the most highly conserved region of CTL2 as consisting of the solvent exposed surface of sheet 1 (Fig 3). The higher conservation observed in the ProFunc analysis reflects the use of 50 of the closest homologs to *C. elegans* CTL2, while the ConSurf analysis was based on the broader set of Piezo homologues selected from those used to generate Fig S1. Consequently, while the same qualitative trends are observed with both programs, ProFunc found a higher residue conservation at this patch compared to calculation done by ConSurf.

Structure of M31R *C. elegans* PIEZO CTL2 domain variant

The single substitution in human PIEZO1 of methionine 2225 to arginine has been linked to the disease Dehydration Hereditary Stomatocytosis (DHS) (Zarychanski et al., 2012). From the multiple sequence alignment of Piezo homologs, we determined that M31 of the *C. elegans* PIEZO CTL2 construct, located in strand 2 of sheet 1, is equivalent to residue M2225 in human PIEZO1 (Fig. S4). Intriguingly, this residue is located in the conserved surface region of CTL2 (Fig. 3). The M31R *C. elegans* mutant CTL2 protein crystallized in a distinct crystal form from the WT domain and the structure was solved by molecular replacement. Overall, the structure of the mutant CTL2 is similar to the WT structure with some minor rearrangements (RMSD Cα = 1.3 Å overall, with 0.7 Å for residues in α-helices and β-strands (Fig. 4a)). In *C. elegans* PIEZO CTL2, M31 is spatially adjacent to a neighboring arginine residue, R94 (Fig. 4b). The most significant change in the M31R mutant CTL2 structure is the shift of the R94 sidechain ~3 Å away from R31, presumably due to electrostatic repulsion (Fig. 4b,c, Fig S5). However, R94 in *C. elegans* PIEZO loop is not conserved in the multiple sequence alignment (Fig. S4). R94 aligns to a glutamate residue that is primarily conserved in the vertebrate Piezo1 and Piezo2. Even though the *C. elegans* PIEZO CTL2 does not have a glutamate at this position, there are three glutamates in proximity to M31: E30, E32, and E98. This results in a net acidic local environment surrounding M31 in the *C. elegans* PIEZO.

Discussion

As a starting point for the structural analysis of Piezo, we have identified a predicted extramembrane domain designated as CTL2 (C-terminal Loop 2) as a promising target for three reasons. (1) There is a moderate degree of sequence conservation in this region through all Piezo homologs, which may imply its significance in the general protein function. (2) We were looking for a target loop with at least 100 amino acids because larger domains are more likely to have a stable core structure. With ~250 residues, CTL2 is the largest conserved loop found among Piezo homologues. Moreover, the boundaries at which this loop starts and ends as defined by different topology prediction methods are similar, simplifying the design of our constructs. (3) A point mutation in the CTL2 domain of human PIEZO1 is found in DHS patients. Removal of this loop, together with the last transmembrane segment and the C-terminal tail, severely impaired the inactivation kinetics of the channel (Bae et al., 2013a), leading to an increased ion influx that may contribute to the disease phenotype (Albuisson et al., 2013; Andolfo et al., 2013; Zarychanski et al., 2012).

The model of CTL2 establishes that the region forms a compact domain containing a beta sandwich with three sheets. The CTL2 fold is apparently unrelated to any other family of proteins, including the β sheet domains present in other eukaryotic channels, specifically the extracellular domains of the two eukaryotic ion channels of known structure (Jasti et al., 2007; Kawate et al., 2009), ASIC (CATH ID: 2.60.470.10) and P2X4 (CATH ID: 2.60.490.10). There is no evidence from either structure of the wild type or M31R mutant that this domain forms a tetramer that might help stabilize the oligomeric state of the intact channel. Mutating the conserved methionine residue into arginine (M31R), corresponding to a human DHS mutation (M2225R), does not cause a significant conformational change in *C. elegans* PIEZO CTL2 domain, suggesting that the effect of this mutation may be to more subtly perturb conformational energetics through changes in electrostatics, or perhaps to interfere with the ability to interact with other domains by changing the interface region.

In conclusion, we have described the first structural characterization of a domain of a eukaryotic mechanosensitive channel, the CTL2 domain of *C. elegans* PIEZO. We have shown that this extramembrane region forms a stable domain that adopts a previously uncharacterized beta sandwich fold. The functional role of this domain in the context of the full length channel remains unclear. In view of the monomeric nature of the CTL2 domain, it is unlikely to mediate tetramerization of the full length channel. As this domain is generally conserved across Piezo homologs, it may have a general role such as mediating proper intracellular trafficking, tethering the intact channel to one or more proteins, or binding of a ligand; the search for binding partners is currently under investigation. The lack of structural similarity between this domain and any known protein fold, including those of eukaryotic and bacterial channels, reinforces the lack of recognizable sequence homology between Piezo and other channels, and highlights the distinctive nature of this enigmatic family of eukaryotic mechanosensitive channels.

Experimental Procedures

Protein cloning and expression

The CTL2 regions from the mouse PIEZO1, mouse PIEZO2, human PIEZO1, *Drosophila* PIEZO and *C. elegans* PIEZO orthologues were cloned into a pET21 vector between the NdeI and XhoI restriction sites, generating a construct with a C-terminal 6xHis tag. The plasmid DNA was transformed into BL-21 gold *E. coli* cells (Stratagene). Cells were grown in Terrific Broth medium until reaching an OD600 of 1.0, when 1 mM IPTG was added. Protein induction was carried on overnight at 20 °C. The CTL2 of *C. elegans* PIEZO (GenBank ID: 392900032) was found to be best suited for structural analysis; the protein and nucleotide sequences of the coding region for this construct are:

MSLLNQIGTISMPEKVTLRISIEGYPPLYEMEAQGSNHDNAELGMIKPDQLASLNQA
LTDSYTTRDTNSILRSRMSVSYLKGYTYEDILIVRFRPESEIYWPISQDSRNAMIDKLS
RNTSVNFEVSLEFTRPYDPNENAALKHSKSWLVPISLDMTIRAKIQSALRGDPGHPIL
IPQSIPAFIQVPNQGELTLPTSIGNTIINDGNPRINTTGMEKSDEARAWFDSLTLNLEQ
GKSQNEKMWIATSEHPGDQNAKLWIKTANTTYSGRPYLQVVGFIDRAFPSLEHHHH
HHATGTCGCTACTCAATCAAATCGGAACTATCAGTATGCCAGAAAAAGTTACGT
TGAGGATTTCGATTGAAGGATATCCACCACTTTACGAGATGGAGGCACAAGGAA
GTAATCACGATAACGCTGAACTTGGAATGATAAAACCTGATCAATTGGCATCTT
TGAATCAAGCATTGACGGATAGTTACACGACACGAGACACTAATTCTATTTTAA
GATCAAGAATGTCTGTATCATATCTGAAAGGATACACATATGAGGATATTCTGA
TTGTGCGATTCCGTCCAGAATCTGAAATTTATTGGCCGATTTCACAGGATTCGAG
AAATGCGATGATCGATAAATTGAGCCGAAACACGTCAGTCAATTTTGAAGTATC
TCTGGAATTCACTCGGCCATATGATCCAAATGAAAACGCTGCTTTAAAACATTC
GAAATCGTGGCTTGTTCCAATCTCCCTGGATATGACGATTCGAGCAAAAATTCaa
AGTGCTCTCCGAGGAGATCCAGGTCATCCGATTCTCATTCCACAGTCAATTCCTG
CGTTTATTCAAGTTCCAAATCAAGGAGAATTGACCCTTCCAACATCAATCGGAA
ATACTATTATCAATGACGGAAATCCACGGATTAATACGACCGGGATGGAAAAAT
CAGACGAAGCTCGGGCTTGGTTCGACTCGTTAACCTTGAATCTCGAACAAGGAA
AATCGCAAAACGAGAAAATGTGGATCGCCACATCCGAACATCCAGGAGACCAA
AATGCGAAACTCTGGATAAAGACTGCAAATACGACGTATTCGGGAAGGCCGTA
CCTTCAAGTTGTCGGATTTATTGATAGAGCATTCCC
ATCACTCGAGCACCACCACCACCACCACTGA

Protein residue numbers are assigned according to their position in this CTL2 construct.

Protein purification

Cells were homogenized in lysis buffer (20 mM Tris-HCl pH 8.0, 50 mM NaCl, lysozyme, DNAse, PMSF) at a ratio of 1 g cells/10 mL of buffer. Cells were lysed using a microfluidizer (Microfluidics, Model M-110L), and the lysate was centrifuged to remove insoluble material. The protein was purified in three steps. First, lysate was run through a NiNTA column, washed with 40 mM imidazole for 15 column volumes, and eluted with 250 mM imidazole. Next, the eluate from the NiNTA column was run through a Superdex-200 16/60 column (GE Healthcare), and the corresponding peak fraction was collected. Finally, the resulting protein fraction was run through an anion exchange column, HiTrap Q

Sepharose FF (GE Healthcare), to obtain the final protein preparation. The identities of the purified wild type (WT) and M31R variant proteins were confirmed by mass spectrometry.

Crystallization & model refinement

WT CTL2 was crystallized by the sitting drop vapor diffusion method against a reservoir containing 0.1 M phosphate-citrate buffer pH 4.0, 26% PEG1000, and 0.2 M Li_2SO_4 at 20 °C in a 96-well plate, at a ratio 0.2 μL protein to 0.2 μL reservoir drop, using intelli sitting drop crystallization plates (ArtRobbins). The protein concentration was 10–12 mg/mL. WT CTL2 crystals appeared after 18 hrs and grew to maturation after 3 days to approximate dimensions of 50 μm × 50 μm × 150 μm. M31R CTL2 was crystallized against a reservoir containing 0.1 M phosphate-citrate buffer pH 4.8, 30% PEG3350, and 0.2 M Li_2SO_4 at 20 °C using similar procedures. These crystals grew more slowly than the WT crystals.

A heavy atom derivative of the WT CTL2 crystals was prepared by soaking in 10 mM potassium tetranitroplatinate (II) for three days, followed by back-soaking in the mother liquor for 2 hrs. Protein crystals were flash frozen in the presence of Fomblin Y 16/6 oil (Sigma), and were sent to the Stanford Synchrotron Radiation Lightsource (SSRL).

Diffraction data were collected at SSRL beamline 12-2 equipped with a PILATUS 6M PAD detector

Diffraction patterns were indexed and integrated using iMOSFLM (Battye et al., 2011) from the CCP4 software package (Potterton et al., 2003) and XDS (Kabsch, 2010). The integrated data was scaled using SCALA (Evans, 2006). Phases for the WT CTL2 were obtained experimentally by Single-wavelength Anomalous Dispersion (SAD) phasing based on the platinum derivative. Five platinum sites were located, and electron density maps were generated using Autosol (Terwilliger et al., 2009) from the PHENIX suite (Zwart et al., 2008). Phases for the M31R CTL2 structure were generated with PhaserMR (McCoy, 2007) by molecular replacement using the WT structure. Model building was done in Coot (Emsley and Cowtan, 2004), and the structure refinements were done using Refmac5 (Murshudov et al., 2011). The final molecular structures were displayed using PyMOL (Schrodinger, 2010).

Supplementary Material

Refer to Web version on PubMed Central for supplementary material.

Acknowledgments

We thank S.E. Kim and A. Patapoutian for providing the *C. elegans* PIEZO construct, S. Hess from the Proteome Exploration Laboratory at the Beckman Institute at the California Institute of Technology for mass spectrometry analysis of the protein crystals, and P. Nikolovski from the Molecular Observatory at the Beckman Institute at the California Institute of Technology. This research was supported by National Institute of Health (NIH GM84211). We acknowledge the Gordon and Betty Moore Foundation, the Beckman Institute, and the Sanofi-Aventis Bioengineering Research Program and the Beckman Institute at Caltech for their generous support of the Molecular Observatory at Caltech. Operations at SSRL are supported by the US DOE and NIH.

References

Albuisson J, Murthy SE, Bandell M, Coste B, Louis-Dit-Picard H, Mathur J, Feneant-Thibault M, Tertian G, de Jaureguiberry JP, Syfuss PY, et al. Dehydrated hereditary stomatocytosis linked to gain-of-function mutations in mechanically activated PIEZO1 ion channels. Nat Commun. 2013; 4:1884. [PubMed: 23695678]

Andolfo I, Alper SL, De Franceschi L, Auriemma C, Russo R, De Falco L, Vallefuoco F, Esposito MR, Vandorpe DH, Shmukler BE, et al. Multiple clinical forms of dehydrated hereditary stomatocytosis arise from mutations in PIEZO1. Blood. 2013; 121:3925–3935. S3921–3912. [PubMed: 23479567]

Ashkenazy H, Erez E, Martz E, Pupko T, Ben-Tal N. ConSurf 2010: calculating evolutionary conservation in sequence and structure of proteins and nucleic acids. Nucleic Acids Res. 2010; 38:W529–533. [PubMed: 20478830]

Bae C, Gnanasambandam R, Nicolai C, Sachs F, Gottlieb PA. Xerocytosis is caused by mutations that alter the kinetics of the mechanosensitive channel PIEZO1. Proc Natl Acad Sci U S A. 2013a; 110:E1162–1168. [PubMed: 23487776]

Bae C, Gottlieb PA, Sachs F. Human PIEZO1: removing inactivation. Biophys J. 2013b; 105:880–886. [PubMed: 23972840]

Bae C, Sachs F, Gottlieb PA. The mechanosensitive ion channel Piezo1 is inhibited by the peptide GsMTx4. Biochemistry. 2011; 50:6295–6300. [PubMed: 21696149]

Battye TG, Kontogiannis L, Johnson O, Powell HR, Leslie AG. iMOSFLM: a new graphical interface for diffraction-image processing with MOSFLM. Acta Crystallogr D Biol Crystallogr. 2011; 67:271–281. [PubMed: 21460445]

Bernsel A, Viklund H, Hennerdal A, Elofsson A. TOPCONS: consensus prediction of membrane protein topology. Nucleic Acids Res. 2009; 37:W465–468. [PubMed: 19429891]

Chalfie M. Neurosensory mechanotransduction. Nat Rev Mol Cell Biol. 2009; 10:44–52. [PubMed: 19197331]

Coste B, Mathur J, Schmidt M, Earley TJ, Ranade S, Petrus MJ, Dubin AE, Patapoutian A. Piezo1 and Piezo2 are essential components of distinct mechanically activated cation channels. Science. 2010; 330:55–60. [PubMed: 20813920]

Coste B, Xiao B, Santos JS, Syeda R, Grandl J, Spencer KS, Kim SE, Schmidt M, Mathur J, Dubin AE, et al. Piezo proteins are pore-forming subunits of mechanically activated channels. Nature. 2012; 483:176–181. [PubMed: 22343900]

Eisenhoffer GT, Loftus PD, Yoshigi M, Otsuna H, Chien CB, Morcos PA, Rosenblatt J. Crowding induces live cell extrusion to maintain homeostatic cell numbers in epithelia. Nature. 2012; 484:546–549. [PubMed: 22504183]

Emsley P, Cowtan K. Coot: model-building tools for molecular graphics. Acta Crystallogr D Biol Crystallogr. 2004; 60:2126–2132. [PubMed: 15572765]

Evans P. Scaling and assessment of data quality. Acta Crystallogr D Biol Crystallogr. 2006; 62:72–82. [PubMed: 16369096]

Faucherre A, Nargeot J, Mangoni ME, Jopling C. piezo2b Regulates Vertebrate Light Touch Response. J Neurosci. 2013; 33:17089–17094. [PubMed: 24155313]

Hofmann K, Stoffel W. TMBASE - A database of membrane spanning protein segments. Biol Chem Hoppe-Seyler. 1993; 374:166.

Holm L, Rosenstrom P. Dali server: conservation mapping in 3D. Nucleic Acids Res. 2010; 38:W545–549. [PubMed: 20457744]

Jasti J, Furukawa H, Gonzales EB, Gouaux E. Structure of acid-sensing ion channel 1 at 1.9 A resolution and low pH. Nature. 2007; 449:316–323. [PubMed: 17882215]

Johns, SJ. TOPO2, Transmembrane protein display software.

Kabsch W. Integration, scaling, space-group assignment and post-refinement. Acta Crystallogr D Biol Crystallogr. 2010; 66:133–144. [PubMed: 20124693]

Kall L, Krogh A, Sonnhammer EL. Advantages of combined transmembrane topology and signal peptide prediction--the Phobius web server. Nucleic Acids Res. 2007; 35:W429–432. [PubMed: 17483518]

Katoh K, Misawa K, Kuma K, Miyata T. MAFFT: a novel method for rapid multiple sequence alignment based on fast Fourier transform. Nucleic Acids Res. 2002; 30:3059–3066. [PubMed: 12136088]

Kawate T, Michel JC, Birdsong WT, Gouaux E. Crystal structure of the ATP-gated P2X(4) ion channel in the closed state. Nature. 2009; 460:592–598. [PubMed: 19641588]

Kelley LA, Sternberg MJ. Protein structure prediction on the Web: a case study using the Phyre server. Nat Protoc. 2009; 4:363–371. [PubMed: 19247286]

Kim SE, Coste B, Chadha A, Cook B, Patapoutian A. The role of Drosophila Piezo in mechanical nociception. Nature. 2012; 483:209–212. [PubMed: 22343891]

Krissinel E, Henrick K. Secondary-structure matching (SSM), a new tool for fast protein structure alignment in three dimensions. Acta Crystallogr D Biol Crystallogr. 2004; 60:2256–2268. [PubMed: 15572779]

Laskowski RA, Watson JD, Thornton JM. ProFunc: a server for predicting protein function from 3D structure. Nucleic Acids Res. 2005a; 33:W89–93. [PubMed: 15980588]

Laskowski RA, Watson JD, Thornton JM. Protein function prediction using local 3D templates. J Mol Biol. 2005b; 351:614–626. [PubMed: 16019027]

Levina N, Totemeyer S, Stokes NR, Louis P, Jones MA, Booth IR. Protection of Escherichia coli cells against extreme turgor by activation of MscS and MscL mechanosensitive channels: identification of genes required for MscS activity. EMBO J. 1999; 18:1730–1737. [PubMed: 10202137]

McCoy AJ. Solving structures of protein complexes by molecular replacement with Phaser. Acta Crystallogr D Biol Crystallogr. 2007; 63:32–41. [PubMed: 17164524]

McHugh BJ, Murdoch A, Haslett C, Sethi T. Loss of the integrin-activating transmembrane protein Fam38A (Piezo1) promotes a switch to a reduced integrin-dependent mode of cell migration. PloS one. 2012; 7:e40346. [PubMed: 22792288]

Murshudov GN, Skubak P, Lebedev AA, Pannu NS, Steiner RA, Nicholls RA, Winn MD, Long F, Vagin AA. REFMAC5 for the refinement of macromolecular crystal structures. Acta Crystallogr D Biol Crystallogr. 2011; 67:355–367. [PubMed: 21460454]

Potterton E, Briggs P, Turkenburg M, Dodson E. A graphical user interface to the CCP4 program suite. Acta Crystallogr D Biol Crystallogr. 2003; 59:1131–1137. [PubMed: 12832755]

Prole DL, Taylor CW. Identification and analysis of putative homologues of mechanosensitive channels in pathogenic protozoa. PloS one. 2013; 8:e66068. [PubMed: 23785469]

Schrodinger, LLC. The PyMOL Molecular Graphics System, Version 1.3r1. 2010.

Schultz J, Milpetz F, Bork P, Ponting CP. SMART, a simple modular architecture research tool: identification of signaling domains. Proc Natl Acad Sci U S A. 1998; 95:5857–5864. [PubMed: 9600884]

Sillitoe I, Cuff AL, Dessailly BH, Dawson NL, Furnham N, Lee D, Lees JG, Lewis TE, Studer RA, Rentzsch R, et al. New functional families (FunFams) in CATH to improve the mapping of conserved functional sites to 3D structures. Nucleic Acids Res. 2013; 41:D490–498. [PubMed: 23203873]

Sonnhammer EL, von Heijne G, Krogh A. A hidden Markov model for predicting transmembrane helices in protein sequences. Proceedings/International Conference on Intelligent Systems for Molecular Biology; ISMB International Conference on Intelligent Systems for Molecular Biology. 1998; 6:175–182.

Terwilliger TC, Adams PD, Read RJ, McCoy AJ, Moriarty NW, Grosse-Kunstleve RW, Afonine PV, Zwart PH, Hung LW. Decision-making in structure solution using Bayesian estimates of map quality: the PHENIX AutoSol wizard. Acta Crystallogr D Biol Crystallogr. 2009; 65:582–601. [PubMed: 19465773]

Zarychanski R, Schulz VP, Houston BL, Maksimova Y, Houston DS, Smith B, Rinehart J, Gallagher PG. Mutations in the mechanotransduction protein PIEZO1 are associated with hereditary xerocytosis. Blood. 2012; 120:1908–1915. [PubMed: 22529292]

Zwart PH, Afonine PV, Grosse-Kunstleve RW, Hung LW, Ioerger TR, McCoy AJ, McKee E, Moriarty NW, Read RJ, Sacchettini JC, et al. Automated structure solution with the PHENIX suite. Methods Mol Biol. 2008; 426:419–435. [PubMed: 18542881]

Highlights

- A conserved loop of the Piezo channel is identified that forms a stable domain.
- The structure of this domain reveals a novel beta sandwich fold.
- The novel fold highlights the distinctive nature of the Piezo channel family.
- A disease related mutation in this domain has minimal structural consequences.

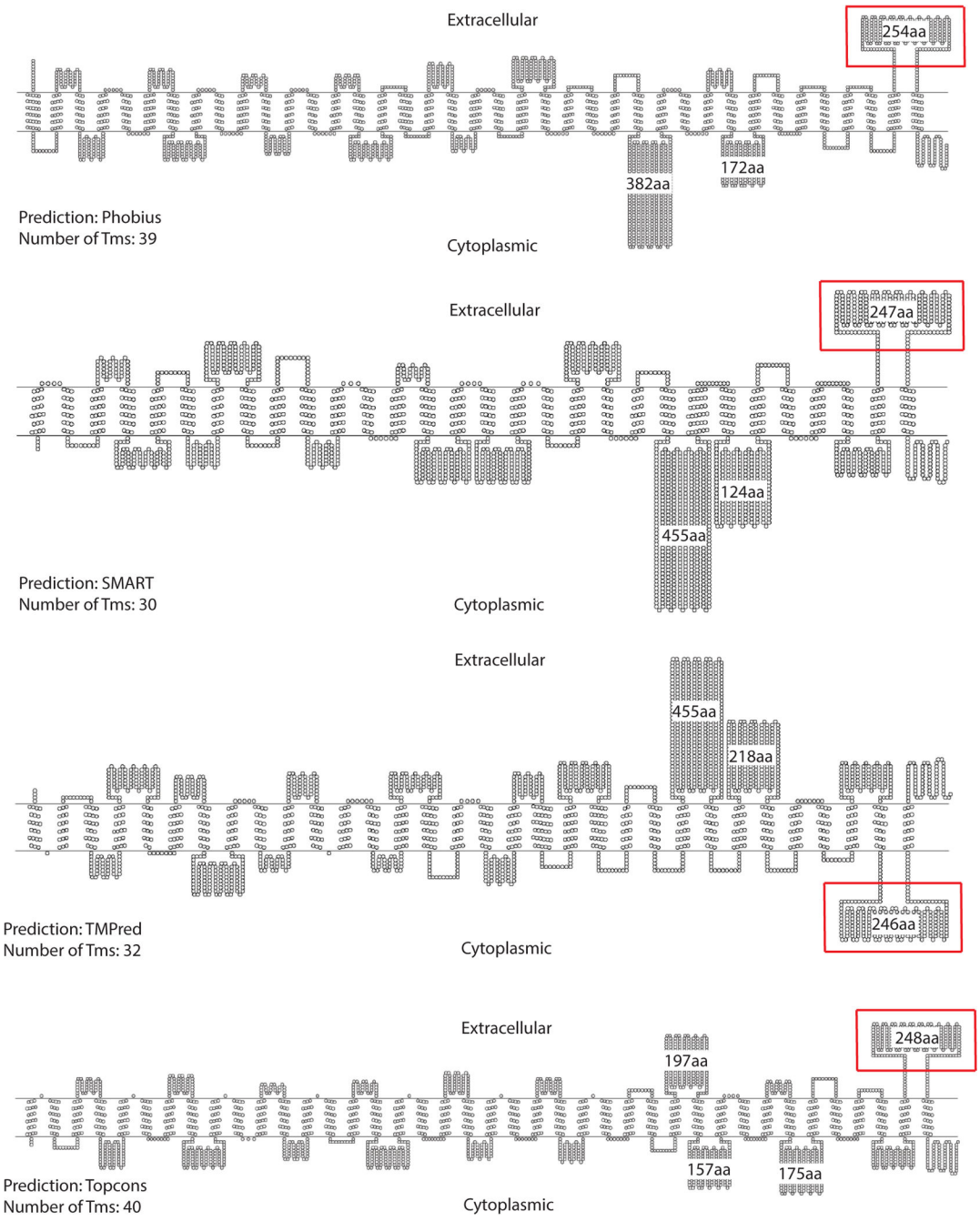

Figure 1. Membrane topology of mouse PIEZO1 as predicted by various membrane topology prediction algorithms

Depending on the membrane topology prediction algorithm, mouse PIEZO1 is predicted to have 30 to 40 transmembrane segments. The numbers of amino acids (aa) for the larger predicted loops are indicated. The loop of interest, CTL2 (red box), is predicted to be extracellular by 3 of the 4 topology prediction algorithms. Since mouse PIEZO1 is the most extensively characterized Piezo channel, it is used to illustrate the topology predictions; Diagrams are drawn using TOPO2 (Johns) http://www.sacs.ucsf.edu/TOPO2/). See also Figure S1.

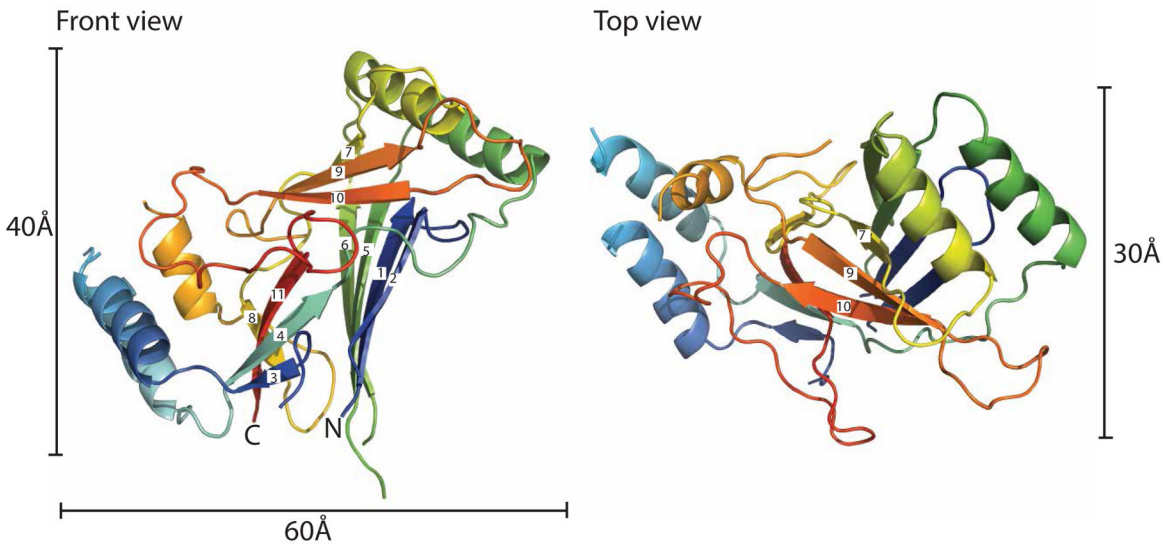

Figure 2. Structure of the wild type *C. elegans* CTL2 domain

The structure of the wild type Piezo CTL2 is colored in a rainbow scheme, progressing from the N-terminus (blue) to C-terminus (red). Front view (left): The loop is oriented so that the connections to the putative transmembrane helices are positioned toward the bottom. The β-strands are numbered sequentially from the N-terminus. Top view (right): the front view, rotated 90° around the horizontal axis. See also Figures S2 and S3.

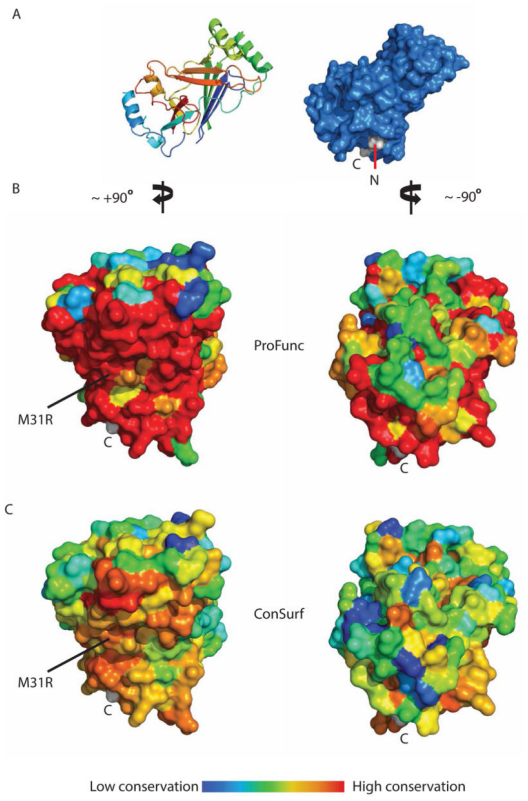

Figure 3. Residue conservation analysis of CTL2

(A) Surface representation of the WT CTL2 domain (marine blue) is oriented in similar fashion to the one displayed in Figure 2 (left side). The N and C terminus are labeled, with the residues colored in light gray. (B) Surface conservation representation from the closest Piezo homologs as calculated by ProFunc (Laskowski et al., 2005a, b) and displayed on the WT CTL2 domain structure. (C) Surface conservation representation from representative Piezo homologs taken from broad branches of eukaryotic kingdom (Fig S1) as calculated by ConSurf (Ashkenazy et al., 2010). The left panels of B and C show the surface of CTL2 upon ~+90° rotation along the y-axis from the view in A, dominated by the solvent exposed surface of sheet 1, while the right panel shows the surface of CTL2 upon -90° rotation from A (180° from the left panels). Surface conservation is colored in a rainbow gradient scheme in such a way that the least conserved region is colored in blue and the most conserved region is colored in red. M31R is located at the conserved sheet 1 surface of CTL2 displayed in the left panels. See also Figures S2 and S4.

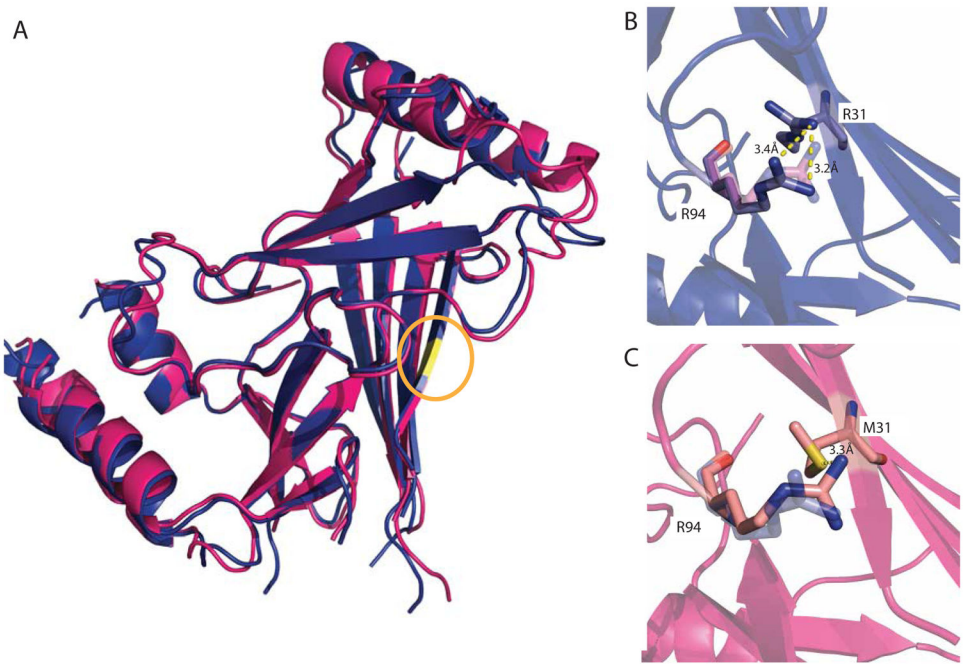

Figure 4. Superposition of wild type and M31R substituted CTL2 domains

(A) Superposition of the wild type (pink) and M31R substituted (blue) CTL2 structures. The position of residue 31 is highlighted in yellow (circled). (B, C). The M31R mutant structure is displayed in blue and the WT structure is displayed in pink; this substitution is accompanied by a modest re-arrangement of the R94 side chain. See also Figure S4 and S5.

Table 1

Data collection and refinement statistics of the wild type and mutant CTL2 domains.

Data set	Wildtype CTL2	CTL2 M31R
Protein Data Bank number	4PKE	4PKX
Data collection statistics		
Space group	H 3 2	P 1 2_1 1
a, b, c (Å)	72.59, 72.59, 241.6	45.18, 37.25, 73.56
β, β, γ (°)	90, 90, 120	90, 91.58, 90
Wavelength (Å)	1.0716	1.0332
Resolution (Å)[a]	33.09 – 2.45 (2.57 – 2.45)	38.97 – 2.54 (2.68 – 2.54)
No. of unique reflection [a]	9377 (1211)	7746 (887)
Mean (I/sigma I) [a]	17.7 (3.0)	28.4 (11.2)
Completeness [a]	99.9% (100%)	93.6% (75.4%)
Average multiplicity [a]	10.1 (10.6)	3.1 (2.8)
Anom. Completeness [a]	99.9% (99.9%)	
DelAnom. correlation between half-sets [a]	0.915 (0.061)	
R-merge [a]	0.093 (0.810)	0.028 (0.085)
Matthew Coefficient	1.951	1.92
Refinement statistics		
Resolution	31.17 – 2.50	33.23 – 2.54
Average B factor (Å^2)	83.9	38.6
R_{work}/R_{free} (%)	22.81/23.84	21.79/25.91
Rmsd bonds (Å)	0.006	0.004
Rmsd angles (°)	1.23	0.97
Ramachandran plot (%)		
Favored	97.5	98.2
Outliers	0	0
Rotamer outliers (%)	5.9	2.9
Molprobity clashscore	13.8	12.8
Molprobity overall score	2.34	1.97

[a]Values in parentheses represents the highest resolution shell